Inorg. Chem. **2006**, *45*, 8136–8143

Structural and Electrochemical Investigations of the High Fluoride Affinity of Sterically Hindered 1,8-Bis(boryl)naphthalenes

Mohand Melaïmi, Stéphane Solé, Ching-Wen Chiu, Huadong Wang, and François P. Gabbaï*

Chemistry TAMU 3255, Texas A&M University, College Station, Texas 77843-3255

Received April 27, 2006

The reaction of 10-bromo-9-oxa-10-boraanthracene with the tetrakis(tetrahydrofuran)lithium salt of dimesityl-1,8-naphthalenediylborate in diethyl ether affords 1-(dimesitylboryl)-8-(10′-bora-9′-oxaanthryl)naphthalene (**2**). This diborane reacts with $[Me_3SiF_2][S(NMe_2)_3]$ to afford the anionic complex [**2**-μ_2-F]$^-$, which has been isolated as a $[S(NMe_2)_3]^+$ salt. The cyclic voltammograms of diborane **2** as well as 1-(dimesitylboryl)-8-(10′-bora-9′-thiaanthryl)naphthalene (**1**) exhibit two reversible reductions at $E_{1/2} = -2.200$ and -2.566 V (vs FcH/FcH$^+$) for **1** and $E_{1/2} = -2.248$ and -2.620 V (vs FcH/FcH$^+$) for **2** corresponding to the sequential reduction of the two boron centers. These two waves simultaneously disappear upon fluoride addition, thus indicating the formation of fluoride chelate complexes [**1**-μ_2-F]$^-$ and [**2**-μ_2-F]$^-$. To identify the origin of the high fluoride affinity displayed by these diboranes, the structures of **2** and [**2**-μ_2-F]$^-$ have been studied experimentally and computationally. The crystallographic studies show that the structure of **2** is distorted, thus indicating the presence of important steric repulsions between the neighboring boryl moieties. By contrast, the structure of the anionic complex [**2**-μ_2-F]$^-$ is much more sterically relaxed than that of **2**, as indicated by a reduction of the B–B distance from 3.279(4) Å in **2** to 2.922(7) Å in [**2**-μ_2-F]$^-$. The structural results suggest that the high fluoride affinity displayed by **2** results, at least in part, from the relief of steric repulsions induced by fluoride binding. Finally, the nature of the bonding as well as the strength of the interactions involved in the B–F–B bridge of [**2**-μ_2-F]$^-$ has been studied using density functional theory calculations and Atoms-In-Molecules analyses. These calculations indicate that the enthalpic gain associated with the formation of two B–F bonds in [**2**-μ_2-F]$^-$ only amounts to a fraction of the energy of a terminal B–F bond. These calculations also suggest that the relief of steric repulsions induced by fluoride binding in **2** may contribute to the high fluoride affinity of these types of molecules.

Introduction

Bidentate boranes including 1,2-diborylbenzenes and 1,8-diborylnaphthalenes have attracted a great deal of interest as receptors for electron-rich substrates.[1−9] It has been clearly demonstrated that such diboranes interact with anionic substrates to form chelate complexes in which the anion bridges the two boron centers. It is generally assumed that the chelate structure of these complexes is largely responsible for their unusual stability. For example, in the case of fluorinated 1,2-diborylbenzene derivatives, some of the resulting anionic complexes are sufficiently stable to coexist with cationic olefin polymerization catalysts.[10,11] Similarly, the hydride complex of 1,8-bis(dimethylboryl)naphthalene fails to reduce benzaldehyde.[12−15]

* To whom correspondence should be addressed. E-mail: gabbai@mail.chem.tamu.edu.

(1) Piers, W. E.; Irvine, G. J.; Williams, V. C. *Eur. J. Inorg. Chem.* **2000**, 2131−2142.
(2) Gabbaï, F. P. *Angew. Chem., Int. Ed.* **2003**, *42*, 2218−2221. Hoefelmeyer, J. D.; Schulte, M.; Tschinkl, M.; Gabbai, F. P. *Coord. Chem. Rev.* **2002**, *235*, 93−103.
(3) Melaimi, M.; Gabbai, F. P. *Adv. Inorg. Chem.* **2005**, *53*, 61−99.
(4) Chen, E. Y.-C.; Marks, T. J. *Chem. Rev.* **2000**, *100*, 1391−1434.
(5) Eisch, J. J.; Kotowicz, B. W. *Eur. J. Inorg. Chem.* **1998**, 761−769.
(6) Williams, V. C.; Piers, W. E.; Clegg, W.; Elsegood, M. R. J.; Collins, S.; Marder, T. B. *J. Am. Chem. Soc.* **1999**, *121*, 3244−3245.
(7) Metz, M. V.; Schwartz, D. J.; Stern, C. L.; Nickias, P. N.; Marks, T. J. *Angew. Chem., Int. Ed.* **2000**, *39*, 1312−1316.
(8) (a) Hergel, A.; Pritzkow, H.; Siebert, W. *Angew. Chem., Int. Ed. Engl.* **1994**, *33*, 1247−1248. (b) Weinman, W.; Hergel, A.; Deforth, T.; Krämer, A.; Pritzkow. H.; Siebert, W. *Z. Naturforsch., B* **1996**, *51b*, 1104−1110.
(9) Reilly, M.; Oh, T. *Tetrahedron Lett.* **1995**, *36*, 221−223.
(10) Williams, V. C.; Irvine, G. J.; Piers, W. E.; Li, Z.; Collins, S.; Clegg, W.; Elsegood, M. R. J.; Marder, T. B. *Organometallics* **2000**, *19*, 1619−1621. Henderson, L. D.; Piers, W. E.; Irvine, G. J.; McDonald, R. *Organometallics* **2002**, *21*, 340−345.
(11) Lewis, S. P.; Taylor, N. J.; Piers, W. E.; Collins, S. *J. Am. Chem. Soc.* **2003**, *125*, 14686−14687.
(12) Katz, H. E. *J. Org. Chem.* **1985**, *50*, 5027−5032.

10.1021/ic060709s CCC: $33.50
Published on Web 08/29/2006

Scheme 1

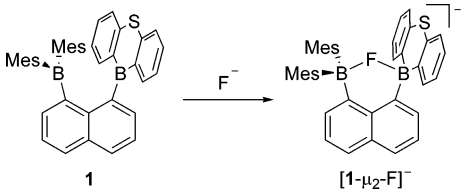

Recent results obtained in our laboratory further substantiate the stabilities of such anionic chelates. Indeed, we recently reported that 1-(dimesitylboryl)-8-(10′-bora-9′-thiaanthryl)-naphthalene (**1**) behaves as a bidentate Lewis acid and readily complexes fluoride to afford the anionic chelate complex [**1**-μ_2-F]$^-$ (Scheme 1).[16] Titration experiments carried out in tetrahydrofuran (THF) indicate that the fluoride binding constant of **1** exceeds 5×10^9 M^{-1}. This binding constant is at least 3 orders of magnitude greater than that measured for the monofunctional boranes including Mes_3B.[16−18] This large difference suggests that the cooperative binding of the anion by the two boron centers may be responsible for the high fluoride affinity of **1**. Because the crystal structure of **1** remains unknown, a careful analysis of the structural reorganization accompanying fluoride binding has not been possible. Since the structural changes induced by fluoride binding may provide additional insight into the high fluoride affinity of such diboranes, we set out to prepare a crystalline diborane, which, along with its fluoride complex, could be structurally studied.

In this paper, we report the synthesis of 1-(dimesitylboryl)-8-(10′-bora-9′-oxaanthryl)naphthalene (**2**), a novel diborane that is a close analogue of **1**. Using both structural and computational techniques, we show that the high fluoride affinity displayed by this novel diborane results, at least in part, from the relief of steric repulsions induced by fluoride binding. Additionally, we demonstrate that the unusual electrochemical properties of **1** and **2** can serve to signal fluoride binding.

Experimental Section

General Procedures. Diborane **1**,[16] tetrakis(tetrahydrofuran)-lithium dimesityl-1,8-naphthalenediylborate,[19] and bis[2-(trimethylsilanyl)phenyl] ether[20] were prepared according to the reported procedures. TASF ($[Me_3SiF_2][S(NMe_2)_3]$) was purchased from Aldrich and used as provided. Chloroform was distilled over CaH_2 and THF over a Na/K amalgam. Air-sensitive compounds were handled under a N_2 atmosphere using standard Schlenk and glovebox techniques. Elemental analyses were performed by Atlantic Microlab (Norcross, GA). All melting points were measured on samples in sealed capillaries and are uncorrected. NMR spectra were recorded on Inova-400 FT NMR (399.63 MHz for ^{1}H, 376.03 MHz for ^{19}F, 128.22 MHz for ^{11}B, and 100.50 MHz for ^{13}C) by using an internal deuterium lock. Chemical shifts, δ, are given in ppm. Spectra are internally referenced to Me_4Si (^{1}H and ^{13}C, $\delta = 0$ ppm) and externally referenced to $BF_3{\cdot}OEt_2$ (^{11}B, $\delta = 0$ ppm), $CFCl_3$ (^{19}F, $\delta = 0$ ppm), and $HgCl_2$ in DMSO (^{199}Hg, $\delta = -1501.6$ ppm).

Table 1. Crystal Data, Data Collection, and Structure Refinement for **2** and [[**2**-μ_2-F][S(NMe$_2$)$_3$]

	2	[**2**-μ_2-F][S(NMe$_2$)$_3$]
	Crystal Data	
formula	$C_{40}H_{36}B_2O$	$C_{46}H_{54}B_2FN_3OS$
M_r	554.31	737.60
cryst size (mm^3)	0.56 × 0.47 × 0.40	0.61 × 0.43 × 0.41
cryst syst	monoclinic	orthorhombic
space group	$P2_1/n$	$Pbca$
a (Å)	16.058(14)	13.579(14)
b (Å)	10.799(10)	12.12(2)
c (Å)	17.637(16)	28.62(3)
β (deg)	100.280(16)	
V (Å^3)	3009(5)	8207(15)
Z	4	8
ρ_{calc} (g cm^{-3})	1.223	1.194
μ (mm^{-1})	0.070	0.122
F(000)	1176	3152
	Data Collection	
T (K)	110(2)	110(2)
scan mode	ω	ω
hkl range	−19 → +17, −12 → +11, −20 → +20	−13 → +15, −23 → +22, −25 → +31
measd reflns	15 328	34 900
unique reflns [R_{int}]	5280 [0.0798]	5822 [0.1066]
reflns used for refinement	5280	5822
	Refinement	
refined param	388	554
R1,[a] wR2[b] [$I > 2\sigma(I)$]	0.0585, 0.1746	0.0753, 0.1528
ρ_{fin} (max/min) (e Å^{-3})	0.569, −0.550	0.951, −0.549

Crystallography. The crystallographic measurements were performed using a Siemens SMART-CCD area detector diffractometer, with graphite-monochromated Mo Kα radiation (λ = 0.710 69 Å). Specimens of suitable size and quality were selected and mounted onto a glass fiber with Apiezon grease. The structures were solved by direct methods, which successfully located most of the non-hydrogen atoms. Subsequent refinement on F^2 using the *SHELXTL/PC* package (version 5.1) allowed location of the remaining non-hydrogen atoms. Further crystallographic details can be found in Table 1.

Electrochemistry. Electrochemical experiments were performed with an electrochemical analyzer from CH Instruments (model 610A) with a glassy-carbon working electrode and a platinum auxiliary electrode. The reference electrode was built from a silver wire inserted into a small glass tube fitted with a porous Vycor frit at the tip and filled with a CH_3CN solution containing nBu$_4$NPF$_6$ (0.3 M) and Ag(NO_3) (0.005 M). All three electrodes were immersed in a deoxygenated THF solution (5 mL) containing nBu$_4$NPF$_6$ (0.3 M) as a support electrolyte and the diborane (**1** or **2**) (0.003 M). The electrolyte was used as purchased. In all cases, ferrocene was used as an internal standard, and all reduction potentials are reported with respect to $E_{1/2}$ of the FcH/FcH$^+$ redox couple.

(13) Katz, H. E. *J. Am. Chem. Soc.* **1985**, *107*, 1420−1421.
(14) Katz, H. E. *Organometallics* **1987**, *6*, 1134−1136.
(15) Katz, H. E. *Inclusion Compd.* **1991**, *4*, 391−405.
(16) Solé, S.; Gabbaï, F. P. *Chem. Commun.* **2004**, 1284−1285.
(17) (a) Yamaguchi, S.; Akiyama, S.; Tamao, K. *J. Am. Chem. Soc.* **2000**, *122*, 6335−6336. (b) Yamaguchi, S.; Shirasaka, T.; Tamao, K. *Org. Lett.* **2000**, *2*, 4129−4132. (c) Yamaguchi, S.; Akiyama, S.; Tamao, K. *J. Am. Chem. Soc.* **2001**, *123*, 11372−11375. (d) Yamaguchi, S.; Shirasaka, T.; Akiyama, S.; Tamao, K. *J. Am. Chem. Soc.* **2002**, *124*, 8816−8817. (e) Kubo, Y.; Yamamoto, M.; Ikeda, M.; Takeuchi, M.; Shinkai, S.; Yamaguchi, S.; Tamao, K. *Angew. Chem., Int. Ed.* **2003**, *42*, 2036−2040.
(18) Liu, Z.-Q.; Fang, Q.; Cao, D.-X.; Wang, D.; Xu, G.-B. *Org. Lett.* **2004**, *6*, 2933−2936.
(19) Hoefelmeyer, J. D.; Gabbaï, F. P. *Organometallics* **2002**, *21*, 982−985.
(20) Gilman, H.; Miles, D. H. *J. Org. Chem.* **1958**, *23*, 1363−1365.

Theoretical Calculations. Density functional theory (DFT) calculations (full geometry optimization) were carried out with *Gaussian03*[21] using the gradient-corrected Becke exchange functional (B3LYP)[22] and the Lee−Yang−Parr correlation functional.[23] A 6-31+g(d′) basis set was used for the boron, oxygen, and coordinating fluorine atoms.[24] A 6-31g basis set was used for all carbon and hydrogen atoms.[25] Frequency calculations, which were carried out on the optimized structure of each compound, confirmed the absence of any imaginary frequencies. Frontier orbitals were obtained from the optimized geometry. The electron density of the DFT-optimized structure of the fluoroborates was subjected to an Atoms-In-Molecules analysis[26] using AIM2000.[27] To calculate the fluoride ion affinity (FIA) of the boranes, the optimized geometries of the boranes and fluoroborates were subjected to a single-point energy calculation using the gradient-corrected Becke exchange functional (B3LYP) and the Lee−Yang−Parr correlation functional and the 6-311+g(2d,p) basis set for all atoms.[28] The fluoride ion affinities were calculated as per eqs 1 and 2. The reaction enthalpies ΔH were derived from the energy of each molecule (from the single-point calculation) corrected to enthalpy by the "thermal correction to enthalpy term" obtained in the frequency calculations.

$$\text{borane} + F^- \xrightarrow[\Delta H]{} \text{fluoroborate} \quad (1)$$

$$\text{FIA} = -\Delta H \quad (2)$$

10-Bromo-9-oxa-10-boraanthracene. This compound has been previously reported.[29] The following synthetic procedure differs from that found in the literature. A solution of boron tribromide (5.5 mL, 45.3 mmol) in dichloromethane (10 mL) was added dropwise under nitrogen to a solution of bis[2-(trimethylsilanyl)-phenyl] ether (5 g, 19.3 mmol) in dichloromethane (20 mL) at −78 °C. This reaction mixture was allowed to warm to room temperature and stirred for 1 h. The solvent was evaporated, and the resulting solid was extracted with diethyl ether (30 mL). This solution was filtered and concentrated. The compound, namely, 10-bromo-9-oxa-10-boraanthracene, crystallized upon cooling to −50 °C. The solvent was removed by filtration, and the crystals were washed with cold diethyl ether (2 × 10 mL) and dried under vacuum. The compound was not purified any further and was used as such for the synthesis of diborane **2**. Yield: 2.84 g (70%). Mp: 104 °C. ^{1}H NMR ($CDCl_3$): δ 7.37 (ddd, 2H, $^3J_{H-H}$ = 7.2 Hz, $^3J_{H-H}$ = 7.6 Hz, $^4J_{H-H}$ = 1.2 Hz, BC−CH−C*H*), 7.54 (dd, 2H, $^3J_{H-H}$ = 8.4 Hz, $^4J_{H-H}$ = 1.2 Hz, OC−C*H*), 7.78 (ddd, 2H, $^3J_{H-H}$ = 7.2 Hz, $^3J_{H-H}$ = 8.4 Hz, $^4J_{H-H}$ = 1.6 Hz, OC−CH−C*H*), 8.32 (dd, 2H, $^3J_{H-H}$ = 7.6 Hz, $^4J_{H-H}$ = 1.6 Hz, BC−C*H*). ^{13}C NMR ($CDCl_3$): δ 117.7, 123.0, 135.4, 135.5 (8C, *C*H), 159.4 (2C, O−*C*). B−*C* was not detected. ^{11}B NMR ($CDCl_3$): δ +52.3.

1-(Dimesitylboryl)-8-(10′-bora-9′-oxaanthryl)naphthalene (2). A solution of 10-bromo-9-oxa-10-boraanthracene (390 mg, 1.50 mmol) in diethyl ether (10 mL) was added to a suspension of tetrakis(tetrahydrofuran)lithium dimesityl-1,8-naphthalenediylborate (670 mg, 1.00 mmol) in diethyl ether (40 mL) at 25 °C. The mixture was stirred 2 h at room temperature, and the solution was filtered. The solvent was removed under vacuum, and the resulting solid was extracted with dichloromethane (20 mL). Following filtration and evaporation of the solvent, the colorless solid was washed with ethanol (2 × 50 mL) and dried under vacuum. This solid was recrystallized from a dichloromethane/hexane (1:1, v/v) mixture, affording colorless crystals of **2**. Yield: 205 mg (37%). Large monocrystals could be obtained by slow evaporation of a diethyl ether solution. Mp: 239 °C. ^{1}H NMR ($CDCl_3$): δ 0.93 (s, 3H, Mes−CH_3), 1.23 (s, 3H, Mes−CH_3), 1.42 (s, 3H, Mes−CH_3), 1.71 (s, 3H, Mes−CH_3), 1.90 (s, 3H, Mes−CH_3), 2.19 (s, 3H, Mes−CH_3), 6.02 (s, 1H, Mes−C*H*), 6.55 (s, 1H, Mes−C*H*), 6.66 (s, 1H, Mes−C*H*), 6.91 (m, 1H, C*H*), 6.95 (m, 1H, C*H*), 7.20 (dd, 1H, $^3J_{H-H}$ = 7.2 Hz, $^4J_{H-H}$ = 1.6 Hz, C*H*), 7.26 (d, 1H, $^3J_{H-H}$ = 8.0 Hz, C*H*), 7.39 (d, 1H, $^3J_{H-H}$ = 8.4 Hz, C*H*), 7.47−7.55 (m, 6H, C*H*), 7.85 (dd, 1H, $^3J_{H-H}$ = 7.2 Hz, $^4J_{H-H}$ = 1.6 Hz, C*H*), 7.99 (dd, 1H, $^3J_{H-H}$ = 7.2 Hz, $^4J_{H-H}$ = 2.4 Hz, C*H*), 8.13 (dd, 1H, $^3J_{H-H}$ = 8.0 Hz, $^4J_{H-H}$ = 1.6 Hz, C*H*). ^{13}C NMR ($CDCl_3$): δ 20.99, 21.05, 22.24, 22.70, 22.97, 25.39 (6C, Mes-*C*H_3), 116.3, 117.1, 120.9, 121.9, 124.6, 125.6, 127.7, 127.9, 129.0, 129.3, 130.1, 131.7, 133.4, 133.8, 135.2, 135.9, 138.4, 140.9 (18C, *C*H), 123.2, 123.7, 138.9, 151.9, 144.6, 147.3 (6C, B-*C*), 134.0, 137.6, 139.9 (2C), 140.9 (2C), 141.5, 143.7 (8C, C−*C*), 159.7, 160.2 (2C, O−*C*). ^{11}B NMR ($CDCl_3$): δ +51.6, +72.4. Anal. Calcd for $C_{40}H_{36}B_2O$: C, 86.67; H, 6.55. Found: C, 86.45; H, 6.52.

Synthesis of [2-μ_2-F][S(NMe$_2$)$_3$]. A solution of TASF (45 mg, 0.16 mmol) in THF (5 mL) was added to a solution of **2** (100 mg, 0.18 mmol) in THF (5 mL) at 25 °C. After 15 min, the solvent was evaporated and the residue was washed with two portions of diethyl ether (20 mL). The remaining white solid was dried under vacuum. Large colorless monocrystals could be obtained by slow evaporation of an acetonitrile solution. Yield: 100 mg (85%). Mp: 238 °C. ^{1}H NMR (acetone-d_6): 1.04 (s, 3H, Mes−CH_3), 1.50 (d, 3H, J_{H-F} = 4.4 Hz, Mes−CH_3), 1.66 (s, 3H, Mes−CH_3), 1.79 (d, 3H, J_{H-F} = 6.0 Hz, Mes−CH_3), 2.00 (s, 3H, Mes−CH_3), 2.06 (s, 3H, Mes−CH_3), 2.97 (s, 18H, NCH_3), 5.90 (s, 1H, Mes−C*H*), 6.17 (m, 2H, C*H*), 6.35 (d, 1H, $^3J_{H-H}$ = 7.2 Hz, C*H*), 6.60 (m, 2H, C*H*), 6.83−6.89 (m, 3H, C*H*), 6.97 (d, 1H, $^3J_{H-H}$ = 7.6 Hz, C*H*), 7.04 (m, 1H, C*H*), 7.08 (dd, 1H, $^3J_{H-H}$ = 6.8 Hz, $^4J_{H-H}$ = 1.2 Hz, C*H*), 7.12−7.18 (m, 2H, C*H*), 7.58 (dd, 1H, $^3J_{H-H}$ = 7.6 Hz, $^4J_{H-H}$ = 1.2 Hz, C*H*), 7.64 (d, 1H, $^3J_{H-H}$ = 8.0 Hz, C*H*). ^{13}C NMR (acetone-d_6): δ 20.77 (d, 2C, J_{C-F} = 3.4 Hz), 24.20 (d, 1C, J_{C-F} = 5.3 Hz), 24.71 (s, 1C), 25.11 (s, 1C), 26.11 (d, 1C, J_{C-F} = 7.2 Hz, Mes−*C*H_3), 38.40 (s, 6C, N*C*H_3), 114.2 (s), 115.4 (d, J_{C-F} = 2.2

(21) Frisch, M. J.; Trucks, G. W.; Schlegel, H. B.; Scuseria, G. E.; Robb, A.; Cheeseman, J. R.; Montgomery, J. A., Jr.; Vreven, T.; Kudin, K. N.; Burant, J. C.; Millam, J. M.; Iyengar, S. S.; Tomasi, J.; Barone, V.; Mennucci, B.; Cossi, M.; Scalmani, G.; Rega, N.; Petersson, G. A.; Nakatsuji, H.; Hada, M.; Ehara, M.; Toyota, K.; Fukuda, R.; Hasegawa, J.; Ishida, M.; Nakajima, T.; Honda, Y.; Kitao, O.; Nakai, H.; Klene, M.; Li, X.; Knox, J. E.; Hratchian, H. P.; Cross, J. B.; Bakken, V.; Adamo, C.; Jaramillo, J.; Gomperts, R.; Stratmann, R. E.; Yazyev, O.; Austin, A. J.; Cammi, R.; Pomelli, C.; Ochterski, J. W.; Ayala, P. Y.; Morokuma, K.; Voth, G. A.; Salvador, P.; Dannenberg, J. J.; Zakrzewski, V. G.; Dapprich, S.; Daniels, A. D.; Strain, M. C.; Farkas, O.; Malick, D. K.; Rabuck, A. D.; Raghavachari, K.; Foresman, J. B.; Ortiz, J. V.; Cui, Q.; Baboul, A. G.; Clifford, S.; Cioslowski, J.; Stefanov, B. B.; Liu, G.; Liashenko, A.; Piskorz, P.; Komaromi, I.; Martin, R. L.; Fox, D. J.; Keith, T.; Al-Laham, M. A.; Peng, C. Y.; Nanayakkara, A.; Challacombe, M.; Gill, P. M. W.; Johnson, B.; Chen, W.; Wong, M. W.; Gonzalez, C.; Pople, J. A. *Gaussian 03*, revision C.02; Gaussian, Inc.: Wallingford, CT, 2004.

(22) Becke, A. *J. Chem. Phys.* **1993**, *98*, 5648−5652.

(23) Lee, C.; Yang, W.; Parr, R. G. *Phys. Rev. B* **1988**, *37*, 785−789. Miehlich, B.; Savin, A.; Stoll, H.; Preuss, H. *Chem. Phys. Lett.* **1989**, *157*, 200−206.

(24) (a) Foresman, J. B.; Frisch, Æ. *Exploring Chemistry with Electronic Structure Methods*, 2nd ed.; Gaussian Inc.: Pittsburgh, PA, 1996; p 100. (b) Hariharan, P. C.; Pople, J. A. *Theor. Chim. Acta* **1973**, *28*, 213−222.

(25) Hehre, W. J.; Ditchfield, R.; Pople, J. A. *J. Chem. Phys.* **1972**, *56*, 2257−2261.

(26) Bader, R. F. W. *Atoms In Molecules: A Quantum Theory*; Oxford University Press: Oxford, U.K., 1990.

(27) AIM 2000: Biegler-König, F. W.; Schönbohm, J.; Bayles, D. *J. Comput. Chem.* **2001**, *22*, 545−549. http://www.aim2000.de.

(28) (a) Krishnan, R.; Binkley, J. S.; Seeger, R.; Pople, J. A. *J. Chem. Phys.* **1980**, *72*, 650−654. (b) Spintzagel, G. W.; Clark, T.; Schleyer, P. v. R.; Hehre, W. J. *J. Comput. Chem.* **1987**, *8*, 1109−1116.

(29) Roth, H. J.; Miller, B. *Arch. Pharm. (Weinheim, Ger.)* **1964**, *297*, 524−528.

Scheme 2 [a]

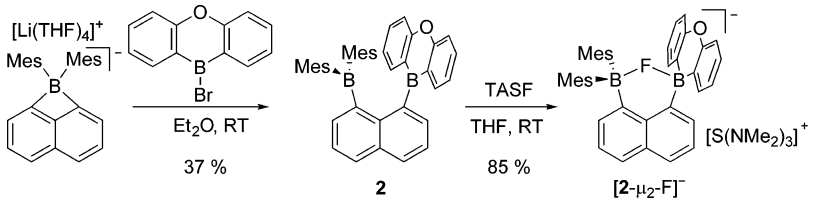

[a] TASF = $[Me_3SiF_2][S(NMe_2)_3]$

Hz), 120.7 (s), 120.8 (s), 124.3 (d, J_{C-F} = 1.9 Hz), 124.9 (s), 125.2 (s), 126.3 (d, J_{C-F} = 2.0 Hz), 126.4 (s), 127.2 (d, J_{C-F} = 3.0 Hz), 128.4 (s), 128.7 (s), 129.3 (s), 129.4 (d, J_{C-F} = 2.0 Hz), 129.7 (d, J_{C-F} = 7.2 Hz), 130.0 (d, J_{C-F} = 8.8 Hz), 137.0 (s), 137.9 (s) (18C, *C*H), 138.8 (s), 133.1 (s), 133.3 (d, J_{C-F} = 2.7 Hz), 140.8 (s), 140.8 (d, J_{C-F} = 2.6 Hz), 140.9 (s), 141.8 (d, J_{C-F} = 6.9 Hz), 142.7 (s), 144.4 (s), 158.9 (s) (10C, C−*C*), 131.4, 134.2, 148.2, 150.4, 151.3, 155.0 (br, 6C, B−*C*). ^{11}B NMR (acetone-d_6): δ +11.7, +17.6. ^{19}F NMR (acetone-d_6): δ −178.6. Anal. Calcd for $C_{46}H_{54}N_3B_2OSF$: C, 74.90; H, 7.38; N, 5.70. Found: C, 73.75; H, 7.34; N, 5.63.

Results and Discussion

Synthesis, Structure, and Characterization of Diborane 2. Diborane **2** was prepared by the reaction of 10-bromo-9-oxa-10-boraanthracene with the Li(THF)$_4$ salt of dimesityl-1,8-naphthalenediylborate[19] and was isolated as a colorless solid in 37% yield (Scheme 2). The properties of this new diborane are close to those of **1**. It is soluble in chloroform, THF, and pyridine. As for **1**, the ^{1}H NMR spectrum of **2** exhibits six distinct resonances that correspond to the aromatic CH groups of the unsymmetrically substituted naphthalene backbone. In addition, four aryl protons and six distinct methyl groups are observed for the mesityl substituents, indicating the existence of a congested structure. The ^{11}B NMR spectrum of **2** shows two resonances at 51.6 and 72.4 ppm, confirming the presence of two different boron centers. This derivative crystallizes in the $P2_1/n$ space group with four molecules per unit cell. The structure of **2** is similar to those of previous diboranes such as 1-(dimesitylboryl)-8-(diphenylboryl)naphthalene (Figure 1 and Table 1).[19] As for other sterically hindered *peri*-substituted naphthalene derivatives, the B1−C1−C9 [128.43(19)°], B2−C8−C9 [129.91(19)°], and C1−C9−C8 [124.23(19)°] angles substantially deviate from the ideal value of 120°. As a result of this steric crowding, the two boron centers are separated by 3.279(4) Å. This separation is much larger than the B−B distance of 3.002(2) Å observed in 1,8-bis(diphenylboryl)-naphthalene, which possesses less sterically demanding aryl substituents.[30] Diborane **2** features a short distance of 2.965-(3) Å between the ipso carbon (C21) atom of one of the mesityl groups and the boron of the 9-oxa-10-boraanthryl unit (B2). This short distance, which is 0.23 Å longer than that observed in the structure of the more Lewis acidic 1-(dimesitylboryl)-8-(borafluorenyl)naphthalene,[31] may indicate the presence of a weak bonding interaction. The slight

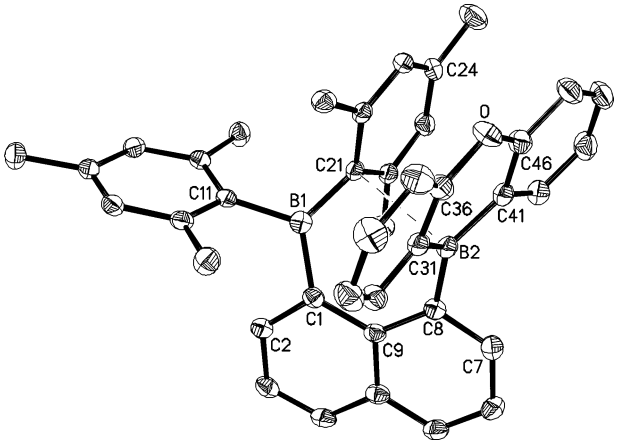

Figure 1. ORTEP view of **2** (50% ellipsoid; hydrogen atoms omitted for clarity). Selected distances [Å] and angles [deg]: B1−C1 1.581(3), B1−C11 1.598(3), B1−C21 1.573(3), B1−B2 3.279(4), B2−C8 1.577(3), B2−C31 1.535(4), B2−C41 1.535(4), B2−C21 2.965(3); C1−B1−C11 117.77-(19), C1−B1−C21 122.55(19), C11−B1−C21 118.52(19), C8−B2−C31 121.6(2), C8−B1−C41 122.1(2), C31−B2−C41 114.2(2), C9−C1−B1 128.43(19), C9−C8−B2 129.91(19), C8−C9−C1 124.23(19).

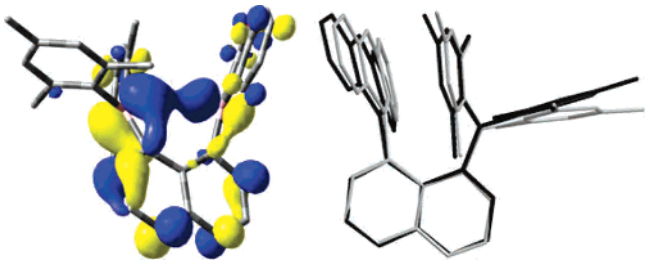

Figure 2. Left: DFT orbital picture showing the LUMO of **2** (isovalue = 0.35). Hydrogen atoms omitted for clarity. Right: overlay representation of theoretical (black) and X-ray (gray) structures for compound **2**.

pyramidalization of the boron center B2 (Σ_{C-B2-C} = 357.9°) as well as the nonlinear B1−C21−C24 angle (170.7°) is in agreement with this view.

Calculated Structure and Electrochemistry of the Diboranes. The structure of **2** was computationally optimized using DFT methods [B3LYP and 6-31+g(d′) for the boron and oxygen atoms and 6-31g for all other atoms]. The optimized geometry of diborane **2** is close to that determined experimentally (Figure 2), although the calculated distance of 3.413 Å separating the boron centers is slightly larger than that observed in the crystal structure [3.279(4) Å]. Examination of the orbitals reveals that the empty boron p orbitals largely contribute to the lowest unoccupied molecular orbital (LUMO; Figure 2) and are oriented toward one another in a transannular fashion.

The cyclic voltammograms of diboranes **1** and **2** are very similar to one another and feature two reversible reduction

(30) Hoefelmeyer, J. D.; Gabbaï, F. P. *J. Am. Chem. Soc.* **2000**, *122*, 9054−9055.
(31) Hoefelmeyer, J. D.; Solé, S.; Gabbaï, F. P. *Dalton Trans.* **2004**, 1254−1258.

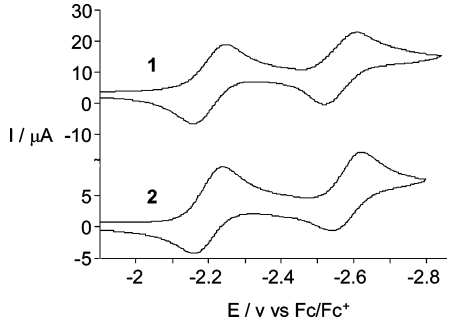

Figure 3. Cyclic voltammograms of **1** ($E_{1/2} = -2.200$ and 2.566 V) and **2** ($E_{1/2} = -2.248$ and -2.620 V) in THF with a glassy-carbon working electrode (0.3 M nBu$_4$PF$_6$). Scan rates: $\nu = 50$ mV s^{-1}.

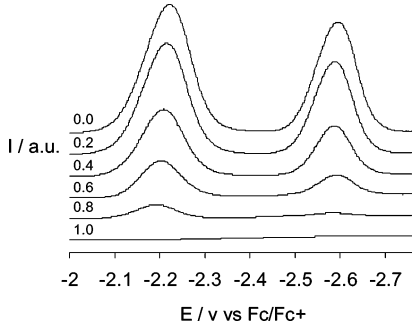

Figure 4. Changes in the differential pulsed voltammogram of **2** observed upon the addition of nBu$_4$F to a THF solution (0.02 M). Similar observations are made for **1**.

waves (Figure 3). The first reduction at $E_{1/2} = -2.200$ V for **1** and $E_{1/2} = -2.248$ V for **2** most likely corresponds to the formation of a radical anion in which the unpaired electron occupies a molecular orbital bearing large contributions from the boron p orbitals.[30,31] The potential for the first reduction of **1** and **2** is markedly more positive than that of other triarylboranes[32−40] such as dimesityl-1-naphthylborane, which is reduced at $E_{1/2} = -2.41$ V (vs FcH/FcH$^+$).[31] The direct σ delocalization of the unpaired electron over the two boron centers can be used to rationalize the observation that **1** and **2** are more easily reduced than dimesityl-1-naphthylborane.[31] The redox behavior of **1** and **2** is reminiscent of that reported for 9,10-dihydro-9,10-dimethyl-9,10-diboraanthracene, whose reduction is facilitated by its antiaromatic character.[41] By analogy with some of our previous investigations,[31] the second reduction wave at $E_{1/2} = -2.566$ V for **1** and $E_{1/2} = -2.620$ V for **2** corresponds to the formation of a dianion, which exists either as a boron−boron σ-bonded derivative or as a diradical. A comparison of the reduction potentials of these two diboranes indicates that **1** is more easily reduced than **2**. Presumably, this phenomenon indicates that the 9-oxa-10-boraanthryl moiety of **2** is more aromatic and, therefore, less electrophilic than the 9-thia-10-boraanthryl moiety of **1**. This effect possibly originates from the lesser amount of mixing of the sulfur p_π orbital with the π system of the boraanthryl moiety in **1**.

Anion Binding. The electrochemical properties of these diboranes directly reflect the coordinative unsaturation of the boron centers. These properties, and more specifically the reduction that these diboranes undergo, should be greatly affected by the binding of nucleophiles to the boron centers. For these reasons, we decided to determine whether cyclic voltammetry and differential pulsed voltammetry could serve to probe anion complexation by these diboranes. To this end, we monitored the cyclic and differential pulsed voltammogram of **1** and **2** upon incremental addition of fluoride, chloride, bromide, iodide, acetate, nitrate, and nitrite. The addition of chloride, bromide, iodide, acetate, nitrate, and nitrite to a THF solution of **1** or **2** containing nBu$_4$PF$_6$ as a supporting electrolyte does not result in any changes in the cyclic voltammogram of **1** and **2**, indicating that these anions do not bind to the diboranes. In contrast, incremental addition of fluoride results in the progressive disappearance of the two reduction waves, which are no longer detected after the addition of 1 equiv of fluoride (Figure 4). These two waves disappear concomitantly and not one after another. The synchronous disappearance of these two waves indicates that fluoride simultaneously binds to the two boron centers of **1** and **2**. This observation further supports the formation of chelate complexes in solution. For all anions, and especially nitrite (p$K_a = 3.29$) and acetate (p$K_a = 4.76$), which are more basic than fluoride (p$K_a = 3.17$), the narrow size of the binding pocket of **1** and **2** is most likely responsible for the observed selectivity. These investigations show that **1** and **2** constitute novel boron-based electrochemical fluoride sensors.[42]

To collect additional evidences for the binding of fluoride to the diboranes, we have also studied the binding of anions by UV−vis spectroscopy in THF. As previously reported for **1**, the addition of fluoride to a THF solution of **2** results in quantitative quenching of the absorption of the diborane at 360 nm ($\epsilon = 16\,000$ mol^{-1} cm^{-1}), indicating the formation of [**2**-μ_2-F]$^-$. The same conclusion is reached by ^{1}H NMR measurements, which show the complete disappearance of the resonance of the free borane and the appearance of broad resonances that can be assigned to the anionic chelate complex. Because of the magnitude of the binding, we have not been able to determine the absolute fluoride binding constant of **2**. Attempts to accurately determine the relative

(32) Krause, E.; Polack, H. *Ber.* **1926**, *59*, 777−785.
(33) Chu, T. L.; Weissman, T. J. *J. Am. Chem. Soc.* **1956**, *78*, 23−26.
(34) Leffler, J. E.; Watts, G. B.; Tanigaki, T.; Dolan, E.; Miller, D. S. *J. Am. Chem. Soc.* **1970**, *92*, 6825−6830.
(35) Eisch, J. J.; Dluzniewski, T.; Behrooz, M. *Heteroatom Chem.* **1993**, *4*, 235−241.
(36) Elschenbroich, C.; Kuhlkamp, P.; Behrendt, A.; Harms, K. *Chem. Ber.* **1996**, *129*, 859−869.
(37) Olmstead, M. M.; Power, P. P. *J. Am. Chem. Soc.* **1986**, *108*, 4235−4236.
(38) Brown, H. C.; Dodson, V. H. *J. Am. Chem. Soc.* **1957**, *79*, 2302−2306.
(39) Weissman, S. I.; van Willigen, H. *J. Am. Chem. Soc.* **1965**, *87*, 2285−2286.
(40) For related studies dealing with the reduction of boranes, see: Kwaan, R. J.; Harlan, C. J.; Norton, J. R. *Organometallics* **2001**, *20*, 3818−3820. Venkatasubbaiah, K.; Zakharov, L. N.; Kassel, W. S.; Rheingold, A. L.; Jäkle, F. *Angew. Chem., Int. Ed.* **2005**, *44*, 5428−5433.
(41) Mueller, P.; Huck, S.; Köppel, H.; Pritzkow, H.; Siebert, W. *Z. Naturforsch., B* **1995**, *50b*, 1476−1484.
(42) Bresner, C.; Aldridge, S.; Fallis, I. A.; Jones, C.; Ooi, L.-L. *Angew. Chem., Int. Ed.* **2005**, *44*, 3606−3609.

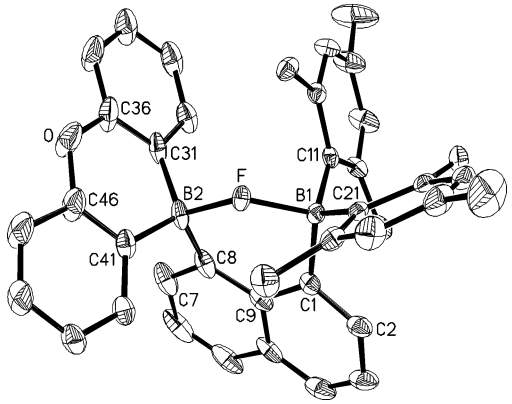

Figure 5. ORTEP view of [**2**-μ_2-F][S(NMe$_2$)$_3$] (30% ellipsoid; hydrogen atoms and the S(NMe$_2$)$_3$ countercation are omitted for clarity). Selected distances [Å] and angles [deg]: B1−F1 1.634(5), B2−F1 1.636(6), B1−C1 1.624(7), B1−C11 1.656 (6), B1−C21 1.646(6), B1−B2 2.922(7), B2−C8 1.617(8), B2−C31 1.597(7), B2−C41 1.615(7); B1−F1−B2 126.6(3), C1−B1−F1 102.0(3), C8−B2−F1 105.9(4), C1−B1−C11 115.8(4), C1−B1−C21 113.7(4), C11−B1−C21 115.9(3), C8−B2−C31 119.1(4), C8−B1−C41 113.0(4), C31−B2−C41 109.2(4), C9−C1−B1 122.5(4), C9−C8−B2 124.7(4), C1−C9−C8 120.9(4).

fluoride binding constants of **1** and **2** have been complicated by the slow kinetics of fluoride exchange between the two receptors.

Isolation and Structural Characterization of the Fluoride Complex of 2. Reaction of **2** with TASF leads to the formation of [**2**-μ_2-F][S(NMe$_2$)$_3$], which has been isolated as a colorless crystalline material. The ^{1}H NMR spectrum of [**2**-μ_2-F]$^-$ differs from that of **2** but is still characteristic of an unsymmetrically substituted naphthalene species. The ^{11}B NMR resonances of [**2**-μ_2-F]$^-$ at 11.7 and 17.6 ppm are in the range expected for tetrahedral boron centers, which is consistent with the coordination of the fluoride anion. The ^{19}F NMR resonance of the bridging fluorine atom appears at −178.6 ppm, which is comparable to the chemical shift observed in other fluoride-bridged species[6] including [**1**-μ_2-F]$^-$.[16]

The [**2**-μ_2-F][S(NMe$_2$)$_3$] salt has been studied by single-crystal X-ray diffraction. Examination of the structure of the anion [**2**-μ_2-F]$^-$ (Figure 5) confirms the presence of a fluorine atom, which bridges the boron centers via B−F bonds of comparable lengths (average 1.635 Å). These bonds are distinctly longer that those formed by the bridging fluorine in [C$_6$F$_4$-1,2-[(BF$_2$)$_2$(μ_2-F)]]$^-$ [average 1.487(4) Å].[43] The accessibility and high Lewis acidity of the difluoroboryl moieties in [C$_6$F$_4$-1,2-[(BF$_2$)$_2$]]$^-$ are probably at the origin of this difference. Nonetheless, a close match is observed between the structure [**2**-μ_2-F]$^-$ and that of [**1**-μ_2-F]$^-$.[16] The B1−F bond of 1.634(5) Å involving the boron center of the dimesityl boryl in [**2**-μ_2-F]$^-$ is almost identical with that measured in [**1**-μ_2-F]$^-$ [1.633(5) Å]. The B2−F bond, which involves the boron atom of the 9-chalcogena-10-boraanthryl fragment, is noticeably longer in [**2**-μ_2-F]$^-$ [1.636(7) Å] than in [**1**-μ_2-F]$^-$ [1.585(5) Å]. This difference indicates that the boron atom of the 9-thia-10-boraanthryl fragment in **1** is a greater Lewis acid than that of the 9-oxa-10-boraanthryl fragment in **2**. This conclusion is in agreement with the observation that the reduction potential of **2** is more negative than that of **1**. As mentioned earlier, this effect most likely originates from the increased aromaticity of the 9-chalcogena-10-boraanthryl moiety in **2** when compared to **1**. As expected from the bridging location of the fluorine atom, B1−F and B2−F bond lengths are significantly longer than that observed in the tris(anthryl)fluoroborate anion (1.47 Å).[17c] The B1−F−B2 angle of 126.6(3)° deviates from the ideal value of 109°, which would be predicted for a sp^3-hybridized fluorine atom. While this distortion may be imposed by the rigid structure, it is important to note that a fluoride anion bridging two triarylboron centers may actually prefer to adopt a linear geometry. Such geometries have been observed in heavier group 13 derivatives such as [(C$_6$F$_5$)$_3$GaFGa(C$_6$F$_5$)$_3$]$^-$.[44] As observed for [**1**-μ_2-F]$^-$, the cooperative binding of the fluoride anion leads to pyramidalization of both boron centers as indicated by the sum of the C−B−C angles ($\sum_{C-B1-C}$ = 345.4°; $\sum_{C-B2-C}$ = 341.3°). Moreover, the C9−C1−B1 [122.5(4)°], C9−C8−B2 [124.7(4)°], and C1−C9−C8 [120.9(4)°] angles in [**2**-μ_2-F]$^-$ are closer to the ideal value of 120° when compared to those in **2** [C9−C1−B1 = 128.43(19)°, C9−C8−B2 = 129.91(19)°, and C1−C9−C8 = 124.23(19)°]. Accordingly, the distance separating the two boron centers B1 and B2 is reduced from 3.279(4) Å in **2** to 2.922(7) Å in [**2**-μ_2-F]$^-$. These structural data suggest that the important steric congestion present in **2** largely disappears in [**2**-μ_2-F]$^-$, where the arylboron substituents adopt a more divergent orientation.

Theoretical Investigation of the Fluoride Complex of 2. The DFT-optimized structure of [**2**-μ_2-F]$^-$ [B3LYP and 6-31+g(d′) for the boron, fluorine, and oxygen atoms and 6-31 g for all other atoms] is close to that determined experimentally (Figure 6). The calculated B1−F (1.64 Å) and B2−F (1.67 Å) bonds are within a few hundreds of an angström from those observed in the crystal [1.634(5) and 1.633(5) Å, respectively]. A very good match is also observed in the B1−F−B2 angle [exptl 126.6(3)°; calcd 126.8°] as well as in the sum of the C−B−C angles ($\sum_{C-B1-C}$: exptl 345.4°; calcd 345.4°. $\sum_{C-B2-C}$: exptl 341.3°; calcd 341.8°). To compare the optimized structure of [**2**-μ_2-F]$^-$ to that of related systems, we optimized the geometry of the simple fluoroborates [**I**-F]$^-$ and [**II**-F]$^-$, whose structures are depicted in Chart 1. For [**I**-F]$^-$ and [**II**-F]$^-$, the B−F bond distances of 1.49 and 1.48 Å are close to that observed experimentally in the tris(anthryl)fluoroborate anion (1.47 Å).[17c] They are also substantially shorter than those computed for [**2**-μ_2-F]$^-$ (average 1.65 Å). Qualitatively, these differences in bond lengths show that the bridging fluorine atom in [**2**-μ_2-F]$^-$ forms weaker B−F bonds than the terminal fluorine atom in [**I**-F]$^-$ and [**II**-F]$^-$. Similar conclusions can be derived from an AIM analysis,[26] which indicates that the values of the densities at the B−F bond critical points in [**2**-μ_2-F]$^-$ [$\rho(r)$ = 0.080 e bohr^{-3} for B1−F and $\rho(r)$ = 0.074 e bohr^{-3} for B2−F] are significantly smaller than those found at the B−F bond critical point of [**I**-F]$^-$ [$\rho(r)$ = 0.126 e

(43) Chase, P. A.; Henderson, L. D.; Piers, W. E.; Parvez, M.; Clegg, W.; Elsegood, M. R. J. *Organometallics* **2006**, *25*, 349−357.

(44) Chen, M.-C.; Roberts, J. A. S.; Marks, T. J. *Organometallics* **2004**, *23*, 932−935.

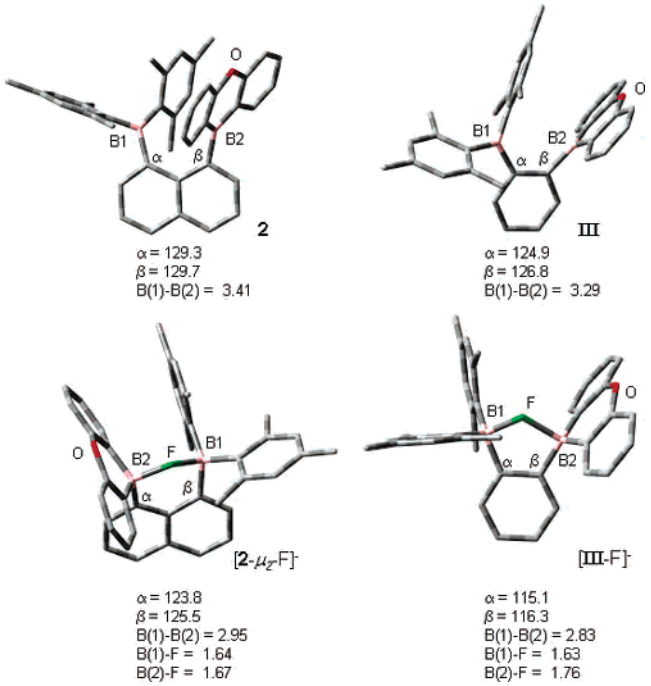

Figure 6. Calculated structures of **2**, **III**, [**2**-μ_2-F]$^-$, and [**III**-F]$^-$.

Chart 1. Borane and Fluoroborate Complexes Studied Theoretically

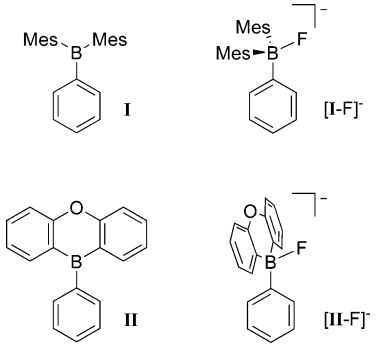

bohr^{-3}] and [**II**-F]$^-$ [$\rho(r)$ = 0.130 e bohr^{-3}]. We also investigated computationally the possible existence of [**I**-F-**II**]$^-$ as a stable gas-phase species. Independently of the starting structures, full geometry optimization always led to complete dissociation of one of the boranes. These results indicate that the stabilization associated with the formation of a B−F−B bridge, if any, is not sufficient to overcome the steric repulsions resulting from the proximity of **I** and **II**. To compare the structure of [**2**-μ_2-F]$^-$ to another model featuring a B−F−B bridge, we computed the structure of [**III**-F]$^-$, in which dimesitylboryl and 9-oxa-10-boraanthryl moieties are linked by an *o*-phenylene backbone (Figure 6). The optimized geometry corresponds to a complex featuring a bridging fluorine atom with B−F bonds of 1.63 and 1.76 Å. The B−F bond of 1.76 Å is noticeably longer than those computed for [**2**-μ_2-F]$^-$. The AIM analysis of [**III**-F]$^-$ indicates that the densities at the B−F bond critical points [$\rho(r)$ = 0.084 e bohr^{-3} for B1−F and $\rho(r)$ = 0.063 e bohr^{-3} for B2−F] are similar to those calculated in [**2**-μ_2-F]$^-$.

To better assess the strength of the interactions involving the bridging fluoride in [**2**-μ_2-F]$^-$ and [**III**-F]$^-$, we have computed the gas-phase FIAs of **I**−**III** and **2**. While different methods for such calculations have been previously published,[45,46] we chose to calculate the FIA of the boranes directly from the energy of the free Lewis acid, F$^-$, and the fluoroborate. To validate our computational approach, we first calculated the FIA of CF_2O. The structures of CF_3O^- and CF_2O were first optimized using the B3LYP functional and 6-31g(d′)/6-31g mixed basis set. The optimized molecules as well as F$^-$ were subsequently subjected to a single-point energy calculation using the B3LYP functional and a 6-311+g(2d,p) basis set for all atoms. The relative enthalpies derived from these single-point energy calculations afforded 48.8 kcal mol^{-1} for the FIA of CF_2O. This value is very close to that experimentally determined (49.9 kcal mol^{-1}),[45] thus pointing to the adequacy of our computational methods. Application of this method to the boranes afforded the following FIAs: 60.74 kcal mol^{-1} for **I**, 64.18 kcal mol^{-1} for **II**, 66.07 kcal mol^{-1} for **III**, and 73.28 kcal mol^{-1} for **2**. These values indicate that the enthalpic gain associated with the formation of two B−F bonds in [**III**-F]$^-$ and [**2**-μ_2-F]$^-$ is relatively small and only amounts to a fraction of the energy of the terminal B−F bond. In other words, the fluoride ion in [**III**-F]$^-$ and [**2**-μ_2-F]$^-$ forms two relatively weak B−F bonds whose cumulated energies only slightly exceed that of the terminal B−F bonds of [**I**-F]$^-$ and [**II**-F]$^-$. Although not as marked as one may have expected, the difference observed in the FIAs of mono- and bifunctional boranes may be responsible for the high fluoride binding displayed by bifunctional boranes such as **2** in solution. In an attempt to understand why **2** has a higher calculated FIA than **III**, we compared the structural changes accompanying fluoride complexation by **III** and **2** (Figure 6). To this end, we examined the C−C−B angles α and β as defined in Figure 6. For **III**, fluoride binding induces changes of the α (124.9° → 115.1°) and β (126.8° → 116.3°) angles around their ideal values of 120°. In the case of **2**, however, the geometry of the free borane is more sterically distorted, as indicated by the elevated values of the α (129.7°) and β (129.3°) angles and the large B−B separation of 3.41 Å. Fluoride binding leads to a decrease of these angles (α = 123.8°; β = 125.5°), which become closer to their ideal values of 120°, indicating a relief of the steric repulsion. Thus, we propose that the important steric congestion present in **2** may, in fact, destabilize the free form of the borane, thus favoring the formation of the less sterically encumbered fluoride adduct. In other words, the high steric compression present between the boryl units of **2** serves to "clamp" the fluoride anion more effectively. This last view is certainly in agreement with the observation of shorter B−F bonds in [**2**-μ_2-F]$^-$ than in [**III**-F]$^-$. Related arguments have been used to explain the unusual basicity of naphthalene-based proton sponges, where the lone pair−lone pair repulsion occurring between the nitrogen atoms serves to destabilize the free base and facilitates its protonation.[47]

(45) Christe, K. O.; Dixon, D. A.; McLemore, D.; Wilson, W. W.; Sheehy, J.; Bootz, J. A. *J. Fluorine Chem.* **2000**, *101*, 151−153.
(46) Krossing, I.; Raabe, I. *Chem.−Eur. J.* **2004**, *10*, 5017−5030.
(47) Peraekylae, M. *J. Org. Chem.* **1996**, *61*, 7420−7425.

Concluding Remarks

The synthetic results presented in this paper further demonstrate the suitability of the $Li(THF)_4$ salt of dimesityl-1,8-naphthalenediylborate as a starting material for the synthesis of asymmetrically substituted 1,8-diborylnaphthalenes. A key aspect of this synthetic method is that it allows for the synthesis of highly sterically hindered derivatives such as **1** and **2**. The steric hindrance present in these diboranes is directly reflected by their NMR spectra as well as by a X-ray single-crystal structure that shows, in the case of **2**, noticeable distortions of the diborane backbone. These diboranes are remarkably selective fluoride anion receptors and fail to interact with bulkier and sometimes more basic anions. The origin of this selectivity possibly results from the narrow size of the binding pocket, which can only accommodate small anions. The formation of the chelate fluoride complexes [**1**-μ_2-F]$^-$ and [**2**-μ_2-F]$^-$ can be readily observed by NMR and UV spectroscopy as well as by cyclic voltammetry and differential pulsed voltammetry. The latter techniques, which show the synchronous disappearance of the reduction waves of the two electroactive boryl moieties upon fluoride addition, confirm the simultaneous coordination of the fluoride anion to both boron centers. Finally, to rationalize the high fluoride affinity of the diboranes described in these studies, we have performed a series of computations on **2** and several model compounds. These calculations indicate that the enthalpic gain associated with the formation of two B−F bonds in fluoride adducts of bidentate Lewis acids is moderate. These calculations also suggest that the relief of steric repulsions induced by fluoride binding in **2** may contribute to the high fluoride affinity of these types of molecules. Ongoing studies are focused on the experimental determination of the enthalpy and entropy changes accompanying fluoride binding in solution.

Acknowledgment. This work was supported by the Welch Foundation (Grant A-1423) and the National Science Foundation (Grant CHE 00-94264, Career Award to F.P.G., and Grant CHE 00-77917, for the purchase of NMR instrumentation). We thank Lisa Perez for her help with the calculations.

Supporting Information Available: Crystallographic data in CIF format for **2** and [**2**-μ_2-F][$S(NMe_2)_3$] and computational details. This material is available free of charge via the Internet at http://pubs.acs.org.

IC060709S